Ultra-Short-Term Offshore Wind Power Prediction Considering Causal Mechanisms Under Typhoons

Junhao Gong
College of Electrical Engineering, Shanghai University of Electric Power, Shanghai, China
gongjunhao1314@163.com

Xiangjing Su
Offshore Wind Power Research Institute, Shanghai University of Electric Power, Shanghai, China
xiangjing_su@126.com

Shuai Yu
College of Electrical Engineering, Shanghai University of Electric Power, Shanghai, China
19186049960@163.com

Lujie Liu
Offshore Wind Power Research Institute, Shanghai University of Electric Power, Shanghai, China
susiellj@163.com

Yuanyuan Liu
College of Electrical Engineering, Shanghai University of Electric Power, Shanghai, China
bzjsh777@qq.com

Yang Fu
Offshore Wind Power Research Institute, Shanghai University of Electric Power, Shanghai, China
mfudong@126.com

***Abstract*—Extreme weather like typhoons causes fluctuations in offshore wind farm power output, seriously endangering the safe operation of power systems. Thus, to address unclear typhoon mechanisms and insufficient spatiotemporal correlation captures, this paper proposes an ultra-short-term offshore wind power prediction considering causal mechanisms under typhoons. Firstly, the traditional Transfer Entropy is modified which quantifies the causal mechanisms between typhoon parameters, meteorological factors, and wind power. Secondly, a Causal-Guided Multi-Attention Spatial-Temporal Graph Attention Network (CM-STGAT) is designed. The model: 1) focuses on key features and historical moments via causal-guided feature and temporal attention, 2) adjusts wind turbine spatial correlation by spatial attention, and 3) fuses spatial-temporal features by alternating Temporal Convolutional Network (TCN) and Graph Attention Network (GAT) stacks. Finally, the effectiveness and superiority of the model is verified with actual measurement data of an offshore wind farm during typhoon scenario in Jiangsu Province, China.**

***Index Terms*--typhoon weather, offshore wind power, causal mechanism, graph neural network, attention mechanism.**

I. Introduction

As global fossil fuel reserves diminish, offshore wind power has emerged as a key pillar in the global energy transition [1]. However, extreme weather events such as typhoons occur frequently in coastal areas, resulting in severe fluctuations to wind power output and endangering the safe operation of power systems [2].

Offshore wind power prediction is a key technology to the current wind power field. Deep learning models such as LSTM [3], TCN [4], and Transformer [5] exhibit excellent performance in processing time-series of offshore wind power. However, when encountering wind power changes under typhoon weather characterized by sudden instantaneous changes, significant fluctuation amplitudes, and complex spatiotemporal correlations, the performances of the traditional deep learning models in capturing complex spatiotemporal features are severely limited.

Current research on wind power prediction mostly relies on complex deep learning models [6]-[7] to mine global features and to improve prediction accuracy. For instance, Wang [8] constructed an integrated model by combining heterogeneous clustering and DALSTM. Aslam [9] proposed a dual-attention mechanism to focus on key temporal and feature information. Sun [10] developed a wind power prediction model by feature sensitivity analysis. However, these methods fail to reveal the essential differences between typhoon and normal weather in predictive modeling, and their complex modeling also fails to characterize the evolutionary mechanisms under extreme weather.

Furthermore, considering geographical locations and wake effects, the state-of-the-art studies have identified a significant spatiotemporal correlation in wind power output. John [11] proposed spatial hierarchical aggregation to optimize prediction. Zhang [12] designed a distributed structure to capture spatiotemporal correlation. Li [13] constructed a directed graph convolutional network to realize spatiotemporal feature fusion. However, these studies ignore that rapid changes in wind conditions will lead to spatiotemporal heterogeneity of wind turbine wake effects, and static graph topology cannot adapt to such dynamic changes. This disconnects the characterization of spatial correlation from the actual typhoon process, resulting in prediction deviations.

To address the above issues, an ultra-short-term offshore wind power prediction considering causal mechanisms under typhoons is proposed. Firstly, the traditional Transfer Entropy is modified to deal with the scenarios of strong typhoon-induced fluctuations. Secondly, we analyze the multi-level

This study is sponsored by the National Key R&D Program of China "Remote monitoring and fault diagnosis technology for offshore wind power grid connected systems （2023YFB2406900）"

979-8-3315-8138-1

causal chains among typhoon parameters, meteorological factors, and wind power. The mechanistic differences between typhoon and normal weather are calculated through causal direction, causal strength, and causal delay. Furthermore, a causal-guided multi-attention spatial-temporal graph attention network (CM-STGAT) is designed to achieve ultra-short-term offshore wind power prediction under typhoons. Finally, case verification is conducted using measurement data from an offshore wind farm in Jiangsu Province, China. The experimental results show that the proposed method effectively improves the accuracy of power prediction.

II. Causal Mechanisms

A. Modification of Transfer Entropy

Transfer Entropy (TE), as an information-theoretic tool, reveals the causal influence between variables by quantifying the predictive gain of the historical information of a source variable on the future state of a target variable [14]. For the discrete series $X=\{x_1,x_2,\cdots,x_N\}$ and $Y=\{y_1,y_2,\cdots,y_N\}$, the traditional TE from X to Y is defined as (1).

$$TE_{X\to Y}=\sum_{y_{n+1},y_n,x_n} p(y_{n+1},y_n,x_n)\log_2\frac{p(y_{n+1}\mid y_n,x_n)}{p(y_{n+1}\mid y_n)} \tag{1}$$

where y_n is the state of the target variable Y at time n.

Traditional TE causality quantification relies on discrete data, matching variable evolution in conventional stationary scenarios [14], yet fails to address the nonlinear, highly abrupt variations in typhoon-related time-series data. To address this issue, modified TE converts continuous sequences $v_i\in[x_i,y_i]$ into multi-value discrete sequences based on data fluctuation patterns according to (2).

$$\tilde{v}_i=sign(\Delta v_i)\cdot[2\mathbb{I}\{|\Delta v_i|\ge\delta_2\}+\mathbb{I}\{\delta_2>|\Delta v_i|\ge\delta_1\}] \tag{2}$$

where δ is the threshold, and $\mathbb{I}\{P\}$ is the indicator function.

Typhoons are complex systems with stochastic delays and historical dependence. However, traditional TE quantifies causal relationships solely based on state associations at adjacent discrete time steps and fails to reasonably constrain the historical state range [14]. Therefore, the delay order τ and the historical dependency order (k,l) need to be introduced into the state vector according to (3). By traversing $\tau\in[1,\tau_{\max}]$ and optimizing (k,l) through grid search, the hysteresis is explicitly captured while ensuring future states rely on a finite set of key historical information.

$$\begin{aligned}\tilde{x}_n^{(k,\tau)}&=\{\tilde{x}_{n-(\tau-1)},\tilde{x}_{n-(\tau-1)-1},\cdots,\tilde{x}_{n-(\tau-1)-k}\}\\ \tilde{y}_n^{(l)}&=\{\tilde{y}_n,\tilde{y}_{n-1},\cdots,\tilde{y}_{n-l}\}\end{aligned} \tag{3}$$

Finally, the modified TE is (4), and it is applicable to offshore wind power systems under typhoons.

$$TE_{X\to Y}^{(k,l,\tau)}=\sum_{y_{n+1},\tilde{y}_n^{(l)},\tilde{x}_n^{(k,\tau)}} p(\tilde{y}_{n+1},\tilde{y}_n^{(l)},\tilde{x}_n^{(k,\tau)})\log_2\frac{p(\tilde{y}_{n+1}\mid\tilde{y}_n^{(l)},\tilde{x}_n^{(k,\tau)})}{p(\tilde{y}_{n+1}\mid\tilde{y}_n^{(l)})} \tag{4}$$

B. Quantification of Causal Mechanisms

If the $TE_{X\to Y}$ stays at a stable level for a long time, there is no causal relationship. If the $TE_{X\to Y}$ has a pronounced peak, and $TE_{X\to Y}>TE_{Y\to X}$ at the delay order moment, the causal direction is $X\to Y$.

When there is a causal relationship $X\to Y$, the maximum value of $T_{X\to Y}$ is taken as the causal strength, and (5) indicates the degree of influence of X on Y.

$$S_{X\to Y}=max(TE_{X\to Y}^{(k,l,\tau)}) \tag{5}$$

The time corresponding to the maximum value of $TE_{X\to Y}$ is taken as the causal delay time, and (6) is used to quantify the causal delay time of $X\to Y$.

$$D_{X\to Y}=argmax_\tau(TE_{X\to Y}^{(k,l,\tau)}) \tag{6}$$

III. Prediction Model with Causal Mechanism

We propose an offshore wind power output prediction model based on a CM-STGAT. Fig.1 illustrates its prediction process, which is detailed as follows.

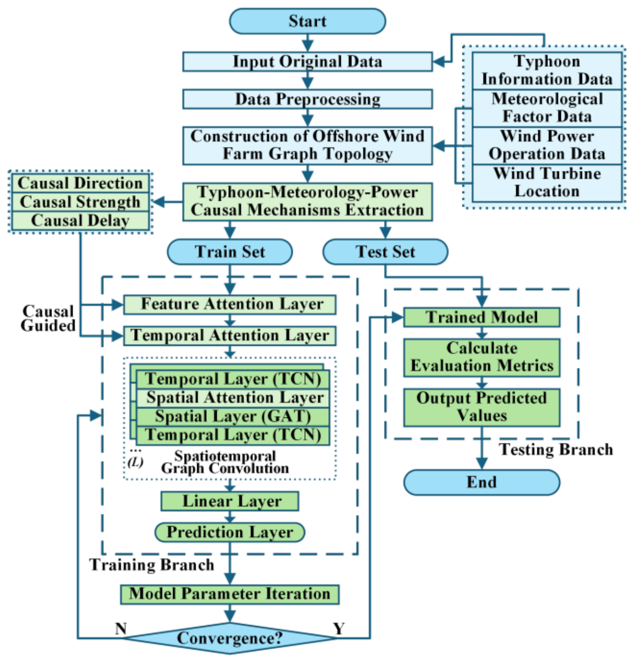

Figure 1. Offshore wind power generation forecasting process

A. Causal-Guided Attention Mechanism

Causal-guided feature and temporal attention mechanisms let the model focus on key driving features and critical historical moments, as illustrated in Fig.2.

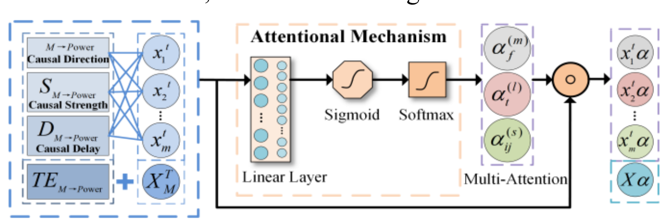

Figure 2. Attention mechanism of causal guidance

The causal relationship $TE_{m\to Power}$ quantitatively describes the information contribution of feature m to future power, which is used to guide the prediction model to focus more on features with high causal strength.

979-8-3315-8138-1

Let the input original feature sequence be $X \in R^{T\times M}$, where M is the number of features. An attention weight $\alpha_f^{(m)}$ is set for each feature m, and the causal strength $S_{m\to Power}$ is incorporated as a prior into the calculation process (7).

$$\alpha_f^{(m)} = softmax\left(\eta \cdot S_{m\to \text{Power}} + v_f^T \cdot \tanh(W_f x^{(m)} + b_f)\right) \quad (7)$$

where v_f, W_f, b_f are learnable parameters, and η controls the guidance strength of the causal prior on the attention weight.

Typhoon influence has an obvious time lag, and temporal attention guided by causal delay time (8) assigns different importance weights $\alpha_t^{(l)}$ to historical time steps.

$$\alpha_t^{(l)} = softmax\left(-\frac{(l - D_{m\to Power})^2}{2\sigma_t^2} + v_t^T \cdot \tanh(W_t x_l' + b_t)\right) \quad (8)$$

where v_t, W_t, b_t are learnable parameters, and σ_t controls the width of the prior distribution of lag time.

B. Construction of Graph Topology and Spatial Attention

This study considers the geographical distance between wind turbines and adjacent wind conditions to construct an offshore wind farm graph topology. Therefore, wind turbines i and j are considered correlated only when their distance is $<\eta_1$ and the Pearson correlation coefficients of their wind speed and direction are both $>\eta_2$.

Spatial correlation of offshore wind power output changes significantly dynamically. The spatial attention mechanism dynamically generates association weights between nodes, enabling the model to adaptively capture dynamic spatial information like time-varying wake effects and heterogeneous wind conditions, and overcome the limitations of traditional static graph topology. For node i and adjacent nodes $N(i) = \{j \mid A_{ij} = 1\}$, its spatial attention weight $\alpha_{ij}^{(s)}$ is (9).

$$\alpha_{ij}^{(s)} = softmax\left(v_{ij}^T \cdot \tanh(W_{ij}\left[x_i^{(s)} \,\|\, x_j^{(s)}\right] + b_{ij})\right) \quad (9)$$

where v_{ij}, W_{ij}, b_{ij} are learnable parameters.

C. Spatial-temporal Graph Convolution

The spatial-temporal graph convolution structure consists of alternately stacked spatial-temporal blocks (ST-Blocks) composed of Temporal Convolutional Network (TCN) and Graph Attention Network (GAT), and is used to capture the nonlinear severe fluctuations and strong spatial-temporal coupling of wind power under typhoon weather.

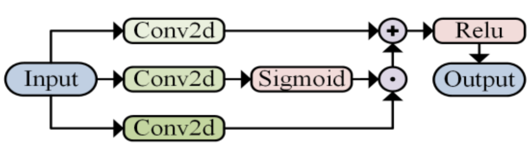

Figure 3. TCN model structure

Temporal convolution independently models the temporal dynamic dependence of power and associated features within each wind turbine node. Fig.3 shows that TCN performs one-dimensional convolution on the feature sequence $H[:,i,:]$ through (10), effectively capturing the long time-lag effect of offshore wind power output under typhoon influence.

$$H_{TCN} = \psi *_d H + b_{TCN} \quad (10)$$

where ψ is the temporal convolution kernel, and $*_d$ is the dilated convolution operation.

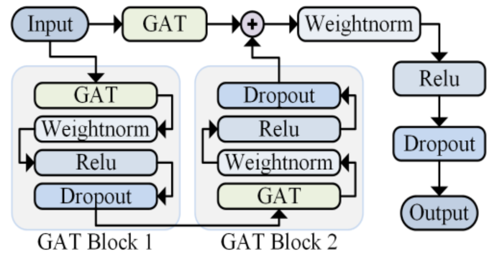

Figure 4. GAT model structure

Spatial convolution aggregates adjacent wind turbine feature information based on dynamic graph topology to characterize spatial dependence. Fig.4 shows GAT performs graph attention convolution over the dynamic spatial graph through (11) to aggregate neighboring nodes information.

$$H_{GAT} = LeakyReLU\left(\sum_{j\in N(i)} \alpha_{ij} \cdot W \cdot H_{TCN}\right) \quad (11)$$

After alternating spatial-temporal convolutions of multiple ST-Blocks, the spatial-temporal feature matrix H_{final} output by the L-th ST-Block is obtained.

Finally, the prediction layer uses a Fully Connected Network (FCN) to map the learned spatial-temporal features to the wind power prediction value (12).

$$\hat{Y} = W_2 \cdot ReLU(W_1 \cdot H_{final} + b_1) + b_2 \quad (12)$$

where W is the fully connected matrix, b is the bias term.

IV. CASE VERIFICATION

A. Case Setup

This study collected historical data from 2018 to 2024 for an offshore wind farm in Jiangsu Province, China. The wind farm consists of 50 turbines with a total installation capacity of 200 MW. The dataset comprises 16 typhoon events and includes features such as typhoon information, meteorological variables, and wind turbine power output.

Data preprocessing involved outlier removal, missing value imputation, and data normalization. Outliers were identified based on the physical operational constraints of the wind power system and were further detected and removed using the DBSCAN algorithm. Subsequently, a Random Forest algorithm was employed to impute all missing data, followed by Min-Max normalization applied to the dataset. Then, data from the 2018 typhoons Ampil and Yagi were selected as the test set, containing 1,864 time steps, while the remaining data formed the training set with 13,892 time steps. All data were sampled at 15-minute intervals.

B. Analysis of Typhoon Causal Mechanisms

To ensure reliable quantification of causal mechanisms in typhoons, the sensitivity of the time window length N in TE calculation must be examined, as it directly governs the coverage of historical information. The $TE(X \to Y)_{max}$ values between partial variables for $N \in [12, 96]$ are shown in Fig.5.

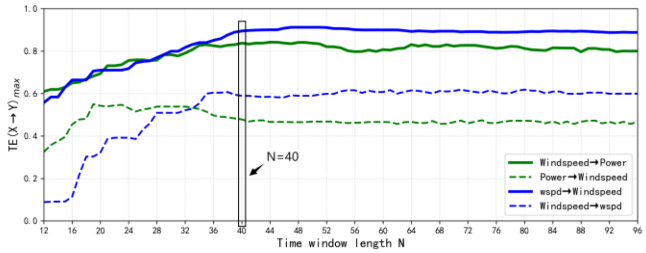

Figure 5. Calculation results of $TE(X\rightarrow Y)_{max}$ with different N

As the N increases, the $TE_{(X\rightarrow Y)}$ fluctuate moderately but consistently satisfy the existence of $TE_{wspd\rightarrow Windspeed} > TE_{Windspeed\rightarrow wspd}$ and $TE_{Windspeed\rightarrow Power} > TE_{Power\rightarrow Windspeed}$, verifying the stable causal chain of local wind speed → wind tower wind speed → output power. When the window length N reaches 40 steps and further increases, the $TE_{(X\rightarrow Y)}$ remain basically stable. Thus, the input data window for TE calculation is set to 40 steps.

TABLE I. DIRECT CAUSAL RELATIONSHIP BETWEEN FEATURES

	$X\rightarrow Y$	$S_{X\rightarrow Y}$	$D_{X\rightarrow Y}$	$X\rightarrow Y$	$S_{X\rightarrow Y}$	$D_{X\rightarrow Y}$
Typhoon Scenario	Direction→wdir	0.4553	3.0	msl→wspd	0.5344	1.0
	Distance→wspd	0.5019	4.0	wspd→swh	0.8576	1.0
	TyPres→TyWind	0.5125	1.0	wdir→Windspeed	0.8513	1.0
	TyDir→wdir	0.4538	4.0	wspd→Windspeed	0.8847	1.0
	TyWind→wspd	0.5518	4.0	swh→Power	0.6634	2.0
	msl→wdir	0.5616	1.0	Windspeed→Power	0.8376	1.0
Normal Weather	msl→wspd	0.4680	1.0	t2m→Power	0.7859	3.0
	msl→wdir	0.4456	1.0	d2m→Power	0.7998	4.0
	wdir→Windspeed	0.8816	1.0	swh→Power	0.5985	4.0
	wspd→Windspeed	0.9106	1.0	Windspeed→Power	0.8241	1.0

Based on the modified TE, the direct causal mechanisms among various features are constructed respectively for both typhoon and conventional meteorological scenarios, as summarized in Table I. These causal mechanisms, along with the input features of this study, are visually presented in Fig.6.

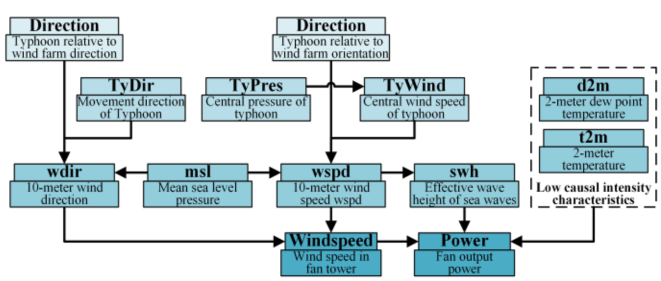

Figure 6. Direct causal relationship between features in typhoon scenarios

In typhoon scenarios, large-scale dynamic factors such as typhoon central pressure, track, and relative distance act as external forcings. They drive changes in local wind speed and direction through the pressure gradient force, with notable delay effects. The causal influence of temperature and humidity on power output is significantly weakened, as the mechanical energy from strong winds far exceeds the effect of air density changes on turbine aerodynamics. The enhanced causality of wave height reflects additional loading from typhoon-driven currents on offshore wind turbine foundations, which directly affects the safe operational limits of turbines.

Fig.7 illustrates the causal mechanism of each feature on the power of offshore wind farms under normal weather and typhoon scenario, intuitively revealing the essential difference between typhoons and conventional weather in predictive model. Typhoon scenario extreme meteorological disturbances dominate the wind energy transfer process, so it is necessary to introduce typhoon characteristic parameters and consider the delay effect in power prediction. Under conventional meteorological conditions, the sea-level pressure gradient drives changes in the local wind field, and the regulation of local thermodynamic properties on air density dominates the wind energy capture efficiency, so its prediction model relies more on local real-time meteorological elements.

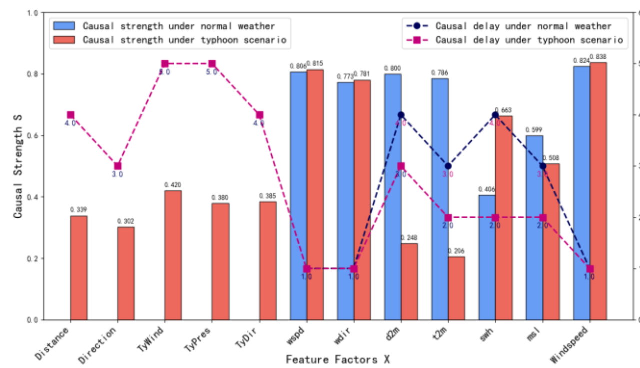

Figure 7. Causal mechanism of each feature on the power of the wind farm

C. Analysis of Prediction Results

This study adopts Root Mean Square Error (RMSE) and Mean Absolute Error (MAE) as error evaluation indicators.

$$RMSE = \sqrt{\frac{1}{N}\sum_{i=1}^{N}(y_i - \hat{y}_i)^2} \tag{13}$$

$$MAE = \frac{1}{N}\sum_{i=1}^{N}\left| y_i - \hat{y}_i \right| \tag{14}$$

where N is the number of samples, $\hat{y}_i$ and y_i are the normalized values of the predicted output and the actual output of the wind farm at time i, respectively.

To validate the effectiveness of the proposed model under typhoon conditions, CM-STGAT is compared with Long Short-Term Memory (LSTM), Gated Recurrent Unit (GRU), Spatio-Temporal Graph Convolutional Network (STGCN), and Dual-Attention Long Short-Term Memory Network (DALSTM). Additionally, an ablation study was conducted by constructing a variant of CM-STGAT without causal mechanisms (M-STGAT). A time window of 20 steps was used to predict the output power at 1-step and 4-step ahead.

Taking the power prediction results of wind turbine No. 40 as an example, the results are shown in Table II. GRU and LSTM fail to capture spatial correlations among wind turbines, leading to the poorest prediction performance. STGCN builds a static graph based on fixed geographical distance, which cannot adapt to the time-varying wake effects caused by abrupt wind direction changes under typhoons. DALSTM relies on data-driven statistical correlations and may introduce spurious correlation features. In contrast, for CM-STGAT, the RMSE and MAE of 1-step prediction are 0.0387 and 0.0369, respectively, while those of 4-step prediction are 0.0925 and

TABLE II. COMPARISON OF PERFORMANCE OF DIFFERENT MODELS

Model	1-Step Forecast		4-Step Forecast		Time Consumption		
	RMSE (10^{-2})	MAE (10^{-2})	RMSE (10^{-2})	MAE (10^{-2})	Total Training Time (s)	Inference Time per Sample (1-Step Forecast) (ms)	Inference Time per Sample (4-Step Forecast) (ms)
GRU	9.17	8.13	18.64	15.98	541	1.55	4.17
LSTM	7.39	6.04	16.03	13.62	628	1.82	4.81
STGCN	5.66	5.54	11.27	10.75	957	2.97	7.82
DALSTM	5.12	4.77	10.70	10.09	1,124	3.51	9.08
CM-STGAT	**3.87**	**3.69**	**9.25**	**8.98**	**1,352**	**4.53**	**11.23**
M-STGAT	4.45	4.12	10.05	9.52	1,186	4.02	10.25

0.0898, which outperform all comparative models. This verifies that the causality-guided feature and temporal dual attention mechanisms can focus on high-contribution feature factors and capture the typhoon delay effect, while the spatial attention can characterize the spatial coupling relationships between wind turbines under typhoons. Meanwhile, compared to CM-STGAT, the prediction performance of M-STGAT degrades. The main reason is that M-STGAT lacks the physical prior constraints from causal mechanisms, making it difficult to effectively select causal features and capture causal delay effects. This indicates that causal guidance enhances the model's ability to focus on physically meaningful features and temporal patterns, thereby improving prediction accuracy.

Regarding computational cost, CM-STGAT requires a longer offline training time of 1,352 s. But in practical use, real-time prediction speed matters more. CM-STGAT achieves prediction time of 4.53 ms for 1-step ahead and 11.23 ms for 4-step ahead, both within an acceptable range.

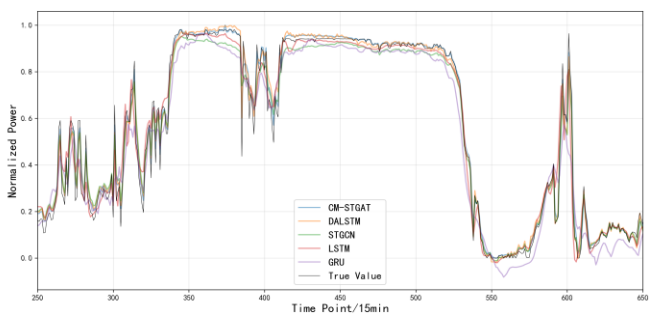

Figure 8. 1-step prediction curves for comparative models

Fig.8 shows the 1-step prediction curves of comparative models. The proposed model exhibits high prediction accuracy in the peak period, trough period, and rapid fluctuation stage of typhoon activity. This indicates that the model can not only identify the temporal dependence but also capture the dynamic spatial correlation in typhoon weather extreme fluctuations.

V. CONCLUSIONS

To address unclear causal mechanisms and difficulty capturing spatiotemporal correlations in offshore wind power prediction under typhoons, this study proposes a CM-STGAT network. Validated on real data from a Chinese offshore wind farm during typhoons, experimental results show that: (1) It effectively quantifies multi-level causal chains among typhoon parameters, meteorological factors and wind power, clarifying the intrinsic mechanistic differences between typhoon and normal weather. (2) The causal-guided attention mechanism directs the model to focus on features and temporal scales with high causal relevance, while the spatial attention mechanism dynamically quantifies inter-turbine spatial correlations. (3) The proposed CM-STGAT outperforms existing models in prediction accuracy, demonstrating its capacity to capture the complex dynamic spatiotemporal characteristics of offshore wind farms under typhoons.

ACKNOWLEDGMENT

This work is supported by National Key R&D Program of China "Remote monitoring and fault diagnosis technology for offshore wind power grid connected systems (2023YFB2406900)".

VI. REFERENCES

[1] P. Kumar, S. Paul, A. K. Saha. "Recent advancements in planning and reliability aspects of large-scale deep sea offshore wind power plants: A review," *IEEE Access*, vol. 13, pp. 3738–3767, Jan. 2025.

[2] J. He, Z. Hu, Y. Liu. "Dispatch strategy for the power system with large offshore wind power integration under a typhoon: A two-stage sample robust optimization approach," *IEEE Transactions on Industry Applications*, vol. 61, pp. 1–13, Jan. 2025.

[3] C. Pan, S. Wen, H. Ye, M. Zhu, S. Jiang. "Deep hedged LSTM network for short term offshore wind power forecasting," in Proc. *2023 IEEE Power & Energy Society General Meeting*, pp. 1–5.

[4] Y. Jin, M. Liu, Z. Lai. "LightWind: A lightweight framework for efficient wind power forecasting," *IEEE Sensors Journal*, vol. 25, pp. 36691-36703, Aug. 2025.

[5] A. Thiyagarajan, B. S. Revathi, V. Suresh. "A deep learning model using transformer network and expert optimizer for an hour ahead wind power forecasting," *IEEE Access*, vol. 13, pp. 33935–33955, Feb. 2025.

[6] Y. Wang, L. Pei. "Short-term wind power prediction method based on multivariate signal decomposition and RIME optimization algorithm," *Expert Systems with Applications*, vol. 259, pp. 125376, Jan. 2025.

[7] J. Gao, P. Chongfuangprinya, Y. Ye, B. Yang. "A three-layer hybrid model for wind power prediction," in Proc. *2020 IEEE Power & Energy Society General Meeting*, pp. 1–5.

[8] S. Wang, X. Kong, N. Wang. "An integrated wind power prediction method based on heterogeneous clustering and DALSTM," in Proc. *2023 IEEE Power & Energy Society General Meeting*, pp. 1–5.

[9] M. Aslam, J. Nam, J. Jung. "An encoder-decoder model with dual-attention mechanism for wind power forecasting," in Proc. *2022 IEEE Power & Energy Society General Meeting*, pp. 1–5.

[10] H. Sun, C. Ye, C. Wan, H. Yao, K. Zhang. "Data-driven day-ahead probabilistic forecasting of wind power based on features sensitivity analysis and meteorological scenario classification," in Proc. *2023 IEEE Power & Energy Society General Meeting*, pp. 1–5.

[11] A. M. John, S. Pant, S. Gupta, Y. Bhardwaj, N. Sharma, A. Gupta. "Spatial hierarchical wind power forecasting," in Proc. 2022 *IEEE Power & Energy Society General Meeting*, pp. 1–5.

[12] Y. Zhang, J. Wang. "A distributed approach for wind power probabilistic forecasting considering spatiotemporal correlation without direct access to off-site information," in Proc. 2*020 IEEE Power & Energy Society General Meeting*, pp. 1–5.

[13] Z. Li, L. Ye, Y. Zhao, M. Pei, P. Lu, Y. Li. "A spatiotemporal directed graph convolution network for ultra-short-term wind power prediction," in Proc. *2024 IEEE Power & Energy Society General Meeting*, pp. 1–5.

[14] T. Tanaka, H. Sandberg, M. Skoglund. "Transfer-entropy-regularized Markov decision processes," *IEEE Transactions on Automatic Control*, vol. 67, pp. 1944–1951, Apr. 2022.

979-8-3315-8138-1